RSC Advances

ROYAL SOCIETY OF CHEMISTRY

www.rsc.org/advances

Journal Name

RSCPublishing

ARTICLE

Co-catalytic mechanism of Au and Ag in silicon etching to fabricate novel nanostructures

Cite this: DOI:

Ruike Li,[a] Meicheng Li,*[ab] Yingfeng Li,[a] Pengfei Fu,[a] Younan Luo,[a] Rui Huang,[a] Dandan Song[a] and Joseph Michel Mbengue[a]

DOI:

www.rsc.org/

Metal-assisted chemical etching is a very popular method of fabricating silicon nanostructures. For the dissolution and recrystallization of Ag, and the inertia of Au, we present a co-catalytic mechanism of silicon etching using non-overlapping Au and Ag nanofilms together, meanwhile, two kinds of novel nanostructures are obtained by changing their up and down positions. It is found that, no matter put the Ag or Au nanofilm on the upper layer, the Ag nanofilm will first participate in reaction, etch the silicon substrate into silicon nanowires (Si NWs). Afterwards, the Au nanofilm will re-etch the Si NWs into thick pillars (Ag upper) or ultrathin porous Si NWs (Au upper). It should be also noted that the vertical etching rates of the two layers don't exhibit observable difference, unlike using them separately, where the vertical etching rate of Ag nanofilm is much higher than that of Au nanofilm. This is because the subsequence re-etching process by the Au nanofilm actually conducts at multi-surfaces, arising from the physical feature that Au can generate excessive holes during the hydrogen peroxide decomposition. Furthermore, this study presents feasible ways for the fabrication of individual thick (~200nm) silicon pillars and ultrathin (~25nm) porous Si NWs. Such insights are of guide significance for the synthesizing of many nanostructures.

Introduction

Silicon nanostructures have attracted a lot of attention in many areas such as microelectronics,[1-3] energy storage,[4] bio-medical devices,[5-7] ultra-sensitive sensors,[8-11] and solar cells.[12-14] The vapor-liquid-solid(VLS) growth has achieved great success in fabricating various silicon nanostructures.31 However, this technology requires high energy consumption, high vacuum and other harsh conditions, and it turn out to be low output and poor reproducibility. To overcome above drawbacks, the metal-assisted chemical etching (MACE) process has been developed, which is gradually becoming one of the most popular methods in fabricating silicon nanostructures. In this technique, the essential reaction occurs between silicon and HF, while the role of the noble metal is to accelerate the reaction.[15-17] Wherein, the noble metal will decompose H_2O_2 and inject holes into silicon substrates through forming a galvanic cell on the metal/silicon interface.

Ag and Au are the noble metals used most popularly. Due to different physical features, they exhibit quite different etching characteristics.[18,19] In the Ag catalytic etching process, the Ag's hole-generating ability just matches its hole-injecting ability; so, the silicon is only etched downwards vertically to sidewall-like smooth Si NWs.[16] While in the Au catalytic etching, since Au can generate excessive holes, porous Si NWs structure will be formed.[22] However, to date there is few report on the etching process using Ag and Au together. Kim et al.[20, 21] have fabricated Si NWs using an Au and Ag bilayer nanofilm. They demonstrate that the Au nanofilm can play the role of protecting the Ag nanofilm, thus using such bilayer can overcome the tapering trend when only use Ag nanofilm. In their work, the bilayer nanofilm is synthesized by template method; therefore, the two layers are completely overlapping thus only the underlying Ag nanofilm plays the catalytic role. If the Au and Ag layers are not overlapping, the etching process should become much more complex, following a co-catalytic mechanism.

In this study, we first compared the vertical etching rates of individual Au and Ag nanofilm. It is found that the vertical etching rate of individual Ag nanofilm is much higher than that of the Au nanofilm. Then, the co-catalytic mechanism of Au and Ag bilayer nanofilm is investigated, by analysing the etching features. We found that during the co-catalytic etching processes of non-overlapping bilayer nanofilms, first, the Ag nanofilm etches the silicon substrate into sidewall-like smooth Si NWs, then, the Au nanofilm re-etches them subsequently. When the Ag nanofilm is the upper layer, thick silicon pillars are obtained; while when the Au nanofilm is the upper one, ultrathin porous Si NWs are obtained. This study can enrich the fundamental principles in MACE, and guide the fabrications of new type of silicon nanostructures.

Experimental

Materials

Silicon wafers (N (100), resistivity of 2-4 Ω•cm) are purchased from China Electronics Technology Group Corporation NO. 46 Research Institute, China. H_2O_2 and HF are purchased from Aladdin Industrial (Shanghai) Co. LTD, Shanghai.

Substrates Preparation

The silicon substrates are prepared in three steps. Firstly, the silicon wafer is cut into 10mm×10mm pieces, and then the silicon pieces are cleaned by acetone, anhydrous ethanol and DI water under ultrasonic condition at room temperature, for 5 min, 5 min and 10 min,

respectively. After that, they are dipped into diluted HF (5mol/L) solution for 5min to remove native oxide. Finally, the cleaned pieces are dried by pure nitrogen gas flow and moved to vacuum drying chamber (60℃) as soon as possible, in order to avoid contamination.

Nanofilm Deposition

Noble metal nanofilms are deposited by magnetron sputtering apparatus (Quorum Q150-TS) after the silicon substrates have been treated by UV for 15min.[23] For the etching process using the Ag or Au nanofilm respectively, their thicknesses are the same, 5nm. For the etching process using the Au and Ag bilayer nanofilm (when Ag covers Au, named Au/Ag bilayer nanofilm; correspondingly, when Au covers Ag, named Ag/Au bilayer nanofilm), the thicknesses of the Ag and Au sub-layer are 4 and 2nm, respectively.

Catalytic etching process

Silicon substrates are dipped into the ternary etchant (HF 5mol/L, H_2O_2 0.5mol/L) after deposited. The etching sustains 5min, at 25℃ maintained by water bath. Finally, the silicon substrates are quickly took out and rinsed with plenty of DI water to remove the residual etchant.

In the etching procedure, galvanic cell is formed on the metal/silicon interface, which can greatly accelerate the etching. The reaction equations[24] are:

Cathode: $H_2O_2+2H^+ \rightarrow 2H_2O+2h^+$ (1)

Anode: $Si+4HF_2^- \rightarrow SiF_6^{2-}+H_2\uparrow+2e^-$ (2)

In this etching process, the holes that generated in the cathodic reduction are attracted to the metal nanofilm by image force and injected into the silicon substrate.[18] Such hole-injection leads to the silicon atoms are oxidized into silica, which can be dissolved by the HF rapidly. The hole-injection mainly occurs at the metal/silicon interface, so the vertical etching rate at this location is much higher than other places.

Characterization

In our study, the morphologies of the nanostructures are characterized by the scanning electron microscope (SEM) (FEI Quanta 200F); and the porous structure on a single silicon nanowire is characterized by the transmission electron microscope (TEM) (ZEISSLIBRA 200 FE).

Results and discussion

To investigate the co-catalytic etching mechanism of the Au and Ag bilayer nanofilm, first, the characteristics etched by individual Ag or Au nanofilm are studied. Then, catalytic etching processes using bilayer nanofilm are carried out, with the Ag or the Au nanofilm on the upper layer; and the results are carefully analysed.

Etching feature using Ag and Au respectively

The respective etching characteristics of the Ag or Au nanofilm are of great help in understanding the co-catalytic mechanism of them together. Fig. 1a and b are the Si NW morphologies etched for 5 min by the Ag and Au nanofilm, respectively. All other experimental conditions are the same (HF 5mol/L, H_2O_2 0.5mol/L, 25℃). The vertical etching rates can be analysed by means of comparing the lengths of the Si NWs.

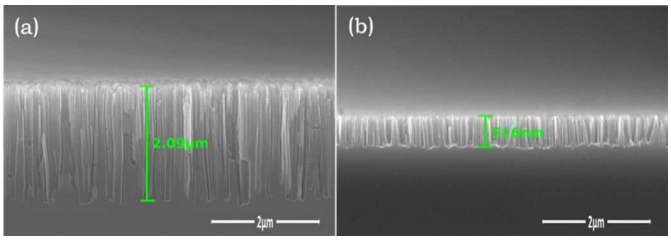

Fig. 1 SEM images of the cross-sectional morphologies etched by individual (a) Ag and (b) Au nanofilm.

We can see that the length of the Si NWs using the Ag nanofilm as catalyst is about 2μm, while the length of Si NWs by the usage of the Au nanofilm is only about 500nm. This denotes that the Ag nanofilm has much better catalytic property than the Au nanofilm. Based on repeated experiments, we have calculated the respective average vertical etching rates of using individual Ag and Au nanofilm as catalyst. As shown in Table 1, their values are 6.91nm/s and 1.78nm/s, respectively.

Table1 Respective vertical etching rate of using individual Ag and Au nanofilm as catalyst

Catalyst	1	2	3	4	5	6	AVG	RMSE
Ag (nm/s)	7.0	6.8	7.2	7.3	6.4	6.8	6.9	0.3
Au (nm/s)	1.8	2.0	1.9	1.6	1.7	1.7	1.8	0.1

The superior catalytic property of the Ag nanofilm can be mainly attributed to that Ag nanofilm can be oxidatively dissolved in H_2O_2, and then recrystallize into nanoparticles. Small particles can contact with the silicon substrate more effectively, therefore, the catalytic activity of the Ag nanofilm can be greatly improved. However, Au is inert against oxidative dissolution, so it can't be dispersed into nanoparticles.[20] The inertia of Au can be directly verified by the fact that, after the etching process, the Au nanofilm can still be observed, as shown in the supplementary information.

Catalytic etching by the Au/Ag bilayer nanofilm

For the etching using bilayer catalyst, the case that Ag nanofilm on the upper layer is first investigated. To understand the etching process, a series of experiments with etching times from 30s to 5min are carried out. The concentrations of the etchant, i.e. the HF and H_2O_2 concentrations, used here are the same as that used in the above section (HF 5mol/L, H_2O_2 0.5mol/L). Fig. 2 shows the SEM images of the cross-sectional morphologies etched for 30s, 1min, 3min and 5 min, respectively.

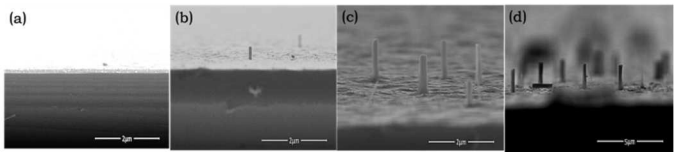

Fig. 2 SEM images of the cross-sectional morphologies etched by the Au/Ag bilayer nanofilm for for (a) 30s, (b) 1min, (c) 3min and (d) 5min.

After 30s, short Si NWs about 200nm height are obtained, as shown in Fig. 2a. Therefore, the vertical etching rate v≈200nm/30s≈6.7nm/s. It should be noted that, this value is very close to that of using individual Ag nanofilm (6.9nm/s). This indicates that in this period, the etching process should be mainly dominated by the Ag nanofilm. Due to the feature that Ag nanofilm can easily be dissolved and recrystallize into nanoparticles, the reasonable etching process in this stage should be shown as in Fig. 3a-c. In this stage, Ag nanofilm first transforms into nanoparticles and penetrate into the interspaces of the Au nanofilm, then etch the silicon substrate into Si NWs. On account of that the vertical etching rate of the Ag nanofilm is much higher that the Au nanofilm as mentioned above, the Au nanofilm should on top of the Si NWs.

After 1 min, from Fig.2b it can be observed that the Si NWs disappear except for some scattering thick pillars with a height of about 400nm. The calculated vertical etching rate 400nm/60s ≈6.7nm/s still closes to the vertical etching rate of using individual Ag nanofilm. It is means that the vertical etching rate is determined by Ag as before. Because of the vertical etching rate of the individual Au nanofilm is much lower than the Ag nanofilm, it can be imagined naturally that there will be sidestep-like structure. However, in practice, there isn't any appearance of sidestep-like structure. This can be rationally explained as follow: Au can generate excessive holes during the H_2O_2 decomposition; so, in the re-etching process conducted by the Au nanofilm, the hole-injection not only occurs at the Au/Si interface, but also occurs at the sidewall nearby; so, the etching actually take place at multi-surfaces simultaneously, as shown in Fig. 3d and e. The multi-surfaces etching can greatly facilitate the vertical etching rate of the Au nanofilm, even catches up with the vertical etching rate of the Ag nanoparticles. As a consequence, almost the whole silicon surface is etched down by the Au nanofilm, except for the big bare locations not covered by any of the Ag or Au nanofilm. This also gives a logical explanation for the disappearance of the Si NWs and the appearance of the sparse pillars.

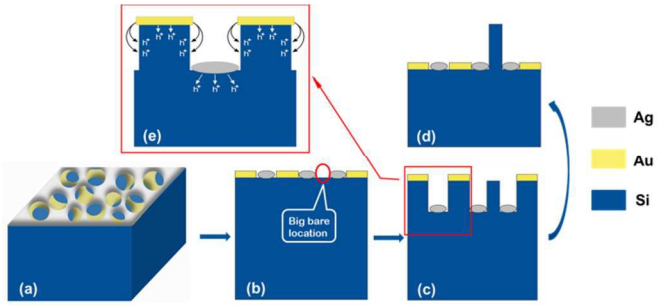

Fig. 3 Illustration of the etching process using the Au/Ag bilayer nanofilm. (a) Au/Ag bilayer nanofilm. (b) The interspaces of the Au nanofilm are filled up by crystallized Ag nanoparticles. (c) Formation of sidewall-like Si NWs. (d) Formation of sporadic Si pillar. (e) Hole-injection process from the Au nanofilm to the Si NWs.

With the increase of etching time from 3min to 5min, the height of the silicon pillars increase gradually, as shown in Fig. 2c and d. The calculated vertical etching rates are about 6.7nm/s and 7.9nm/s, respectively, which are also consistent with the above obtained rate by Ag etching.

The thick Si pillars we fabricated can be used as substrate for the growth of carbon nanotubes[25, 32-34] and Cu nanofilms.[26] In addition, they may have great potential in broadband heterojunction photodetector manufacturing engineering as well.[27-28]

Catalytic etching by the Ag/Au bilayer nanofilm

We also carried out experiments that etching the silicon substrate by the Ag/Au nanofilm for 5min. Because the Ag nanofilm is beneath the Au nanofilm, the etching area of the Ag nanofilm is no longer depends on the apertures of the Au nanofilm in the initial stage. The actual etching process should be a kind of double-screen process by the Ag and Au nanofilm, as shown in Fig.4: the Ag nanofilm first etches the silicon into vertical sidewall-like smooth Si NWs; soon afterwards, the Au nanofilm re-etches the Si NWs into ultrathin porous Si NWs.

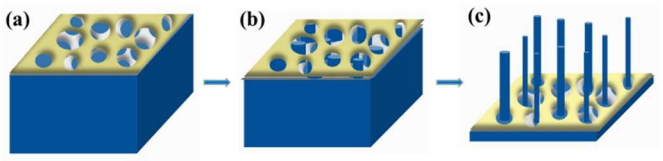

Fig. 4 The schematic diagram of the Ag/Au nanofilm catalytic etching process. (a) The Ag/Au bilayer nanofilm. (b) The crystallized Ag nanoparticles etch the silicon substrate into sidewall-like Si NWs. (c) The Au nanofilm re-etches the Si NWs into ultrathin porous Si NWs.

The etching morphology is given in Fig. 5a. Homogeneous ultrathin Si NWs are obtained. The average diameter of them is about 25 nm, which can be ascribed to the double-screen effect. The much bigger density of the Si NWs than those etched by the Au/Ag nanofilm, clearly denote the much different etching mechanism. From the HRTEM image of the surface of an individual nanowire, as shown in Fig. 5b, we can see that the nanowire is covered by dense and homogeneous nanoscale pores. These pores, marked by red dotted circles, are of diameter about 2nm. The formation of these pores is due to the catalytic etching effect of the Au nanofilm. Metal's catalytic activity is related to its ability of decomposing H_2O_2 and seizing electrons from silicon. In the etching stage by Ag, the hole-generating ability of cathodic reduction reaction just matches its hole-injecting ability. Therefore, silicon substrate will be only etched vertically, leading to the formation of sidewall-like Si NWs. Coming to the Au etching stage, because Au's hole-generating ability is much stronger than its hole-injecting ability, excessive holes will exist. These excessive holes can escape the image force of the Au nanofilm, diffuse to the sidewall of the Si NWs. i.e. the hole-injection not only occurs in the Au/Si interface, but also occurs on the sidewall of the Si NWs. The hole-injection on the sidewall leads to the formation of the pores.

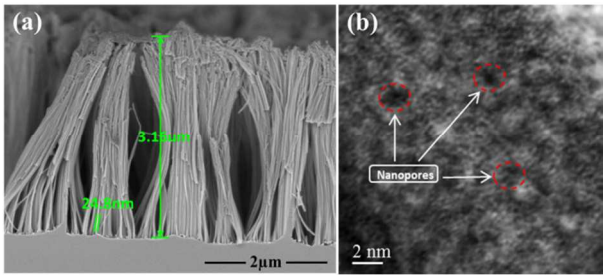

Fig. 5(a) SEM image of the cross-sectional morphology of ultrathin porous Si NWs. (b) HRTEM image of the surface of a single ultrathin porous Si NW.

The ultrathin porous Si NWs may have great potential in a wide range of applications due to their ultrathin and porous properties. For example, both of these features can greatly improve lithium batteries' ability of storing electric charges.[29-30]

Conclusions

In summary, the co-catalytic etching mechanism is due to the synergetic action of the Ag and Au assisted etching. The quick etching feature of Ag can effectively complement the inertia of Au, bring in the first etching of the silicon into nanowires catalysed by Ag film; and then, the excellent hole-generating ability of Au will bring in 3D etching of Si NWs, which results in high vertical etching rate, so the later extraordinary nanostructures are formed. In detail, the Ag nanofilm first takes part in the etching process, then the Au nanofilm conducts the subsequent etching procedure. In the initial step, the Ag nanofilm etches the silicon substrate downwards to form sidewall-like Si NWs. In the latter step, when the Ag nanofilm is on the upper layer, thick silicon pillars are obtained; when the Ag nanofilm is in the lower layer, ultrathin porous Si NWs are obtained. Notably, the vertical etching rates of the two layers don't show up observable difference, unlike using them separately, where the vertical etching rate of the Ag nanofilm is much higher than that of the Au nanofilm. We attribute this synchronism to the fact that Au can generate excessive holes during the H_2O_2 decomposition; so that the hole-injection not only occurs at the Au/Si interface but also at the sidewall nearby, in the re-etching process. That is to say, the Au nanofilm actually conducts a multi-surfaces etching simultaneously. The mechanisms we interpreted could give an inspiring instruction to a wide range of nanostructure fabrications. And this study also provides feasible ways to fabricate single silicon pillars and ultrathin porous Si NWs.

Acknowledgements

This work is supported partially by National High-tech R&D Program of China (863 Program, No. 2015AA034601), National Natural Science Foundation of China (Grant nos. 91333122, 51402106, 51372082, 51172069, 61204064 and 51202067), Ph.D. Programs Foundation of Ministry of Education of China (Grant nos. 20120036120006, 20130036110012), Par-Eu Scholars Program, and the Fundamental Research Funds for the Central Universities.

Notes and references

[a] State Key Laboratory of Alternate Electrical Power System with Renewable Energy Sources, North China Electric Power University, Beijing, 102206, China.
E-mail: mcli@ncepu.edu.cn
[b] Chongqing Materials Research Institute, Chongqing, 400707, China.

† Electronic Supplementary Information (ESI) available: SEM image of no existence of the Ag nanofilm, SEM image of existence of the Au nanofilm. See DOI:

1 G. D. Yuan, Y. B. Zhou, C. S. Guo, W. J. Zhang, Y. B. Tang, Y. Q. Li,Z. H. Chen, Z. B. He, X. J. Zhang, P. F. Wang, I. Bello, R. Q. Zhang, C. S.Lee and S. T. Lee, *ACS. Nano,* 2010, 4, 3045-3052.
2 Y. Cui and C. M. Lieber, *Science*, 2001, 291, 851-853.
3 L. J. Chen, *J. Mater. Chem.*, 2007, 17, 4639-4643.
4 K. Peng, J. Jie, W. Zhang and S. T. Lee, *Appl. Phys. Lett.*, 2008, 93, 033105.
5 B. H. Zhang, H. S. Wang, L. H. Lu, K. L. Ai, G. Zhang and X. L. Cheng, *Adv. Funct. Mater.*, 2008, 18, 2348-2355.
6 S. Wang, H. Wang, J. Jiao, K. Chen, G. E. Owens, K. Kamei, J. Sun, D. J. Sherman, C. P. Behrenbruch, H. Wu and H. Tseng, *Angew. Chem. Int. Ed.*, 2009, 48, 8970-8973.
7 M. L. Zhang, C. Q. Yi, X. Fan, K. Q. Peng, N. B. Wong, M. S. Yang, R. Q. Zhang and S. T. Lee, *Appl. Phys. Lett.*, 2008, 92, 043116.
8 Y. Cui, Q. Wei, H. Park and C. M. Lieber, *Science*, 2001, 293, 1289-1292.
9 M. W. Shao, H. Yao, M.L. Zhang, N. B. Wong, Y. Y. Shan and S.T. Lee, *Appl. Phys. Lett.*, 2005, 87, 183106.
10 G. F. Zheng, F. Patolsky, Y. Cui, W. U. Wang and C. M. Lieber, *Nat. Biotechnol.*, 2005, 23, 1294-1301.
11 F. Patolsky, B. P. Timko, G. H. Yu, Y. Fang, A. B. Greytak, G. F. Zheng and C. M. Lieber, *Science*, 2006, 313, 1100-1104.
12 M. D. Kelzenberg, S. W. Boettcher, J. A. Petykiewicz, D. B. Turner-Evans, M. C. Putnam, E. L. Warren, J. M. Spurgeon, R. M. Briggs, N. S. Lewis and H. A. Atwater, *Nat. Mater.*, 2010, 9, 239-244.
13 F. Bai, M. C. Li, R. Huang,Y. F. Li, M. Trevor and K. P. Musselman, *RSC Adv.*, 2014, 4, 1794-1798.
14 Y. F. Li, M. C. Li, R. K. Li, P. F. Fu, L. H. Chu and D. D. Song, *Appl. Phys. Lett.*, 2015, 106, 091908.
15 F. Bai, M. C. Li, R. Huang, D. D. Song, B. Jiang and Y. F. Li, *Nanoscale. Res. Lett.*, 2012, 7, 557.
16 F. Bai, M. C. Li, D. D. Song, H. Yu, B. Jiang and Y. F. Li, *J. Solid. State. Chem.*, 2012, 196, 596-600.
17 F. Bai, M. C. Li, P. F. Fu, R. K. Li, T. S. Gu, R. Huang, Z. Chen, B. Jiang and Y. F. Li, *APL. Mater.*, 2015, 3, 056101.
18 M. K. Dawood, S. Tripathy, S. B. Dolmanan, T. H. Ng, H. Tan and J. Lam, *J. Appl. Phys.*, 2012, 112, 073509.
19 M. A. Lachiheb, N. Nafie, M. B. Rabha and M. Bouaïcha. *Phys. Status. Solidi. C.*, 2014, 11, 337-343.
20 J. Kim, H. Han,Y. H. Kim, S. H. Choi, J. C. Kim and W. Lee, *Acs. Nano*, 2011, 5, 3222-3229.
21 J. Kim, Y. H. Kim, S. H. Choi and W. Lee, *ACS. Nano*, 2011, 5, 5242-5248.
22 C. L. Lee, K. Tsujino, Y. Kanda, S. Ikeda, M. Matsumura, *J. Mater. Chem.*, 2008, 18, 1015-1020.
23 F. Bai，M. C. Li，R. Huang，Y. Yu，T. S. Gu，Z. Chen，H. Y. Fan and B. Jiang, *J. Nanopart. Res.*, 2013, 15, 1915-1921.
24 D. Wang, R. Ji, S. Du, A. Albrecht and P. Schaaf, *Nanoscale. Res. Lett.*, 2013, 8:42.
25 H. S. Uh and S. Park, *Diam. Relat. Mater.*, 2015, 54, 74-78.
26 X. H. Yang, Z. G. Chen, W. F. Jiang, F. G. Zeng and X. J. Li, *Mat. Sci. Semicon. Proc.*, 2013, 16, 747-751.
27 W. T. Lai, P. H. Liao, A. P. Homyk and A. Scherer, *IEEE Photonic. Tech. L. Lett.*, 2013, 25, 1520-1523.
28 M. Melvin, D. Kumar, J. H. Yun and J. Kim, *Infrared. Phys. Tech.*, 2015, 69, 174-178.
29 H. C. Tao, L. Z. Fan and X. H. Qu, *Electrochim. Acta.*, 2012, 71, 194-200.
30 X. F. Chen, Y. Huang, J. J. Chen, X. Zhang, C. Li and H. J. Huang, *Ceram. Int.*, 2015, 41, 8533-8540.
31 S. H. Lee, T. Lee, K. Moon and J. M. Myoung, *ACS Appl. Mater. Inter.,* 2013, 5, 11777−11782.

32 P. Zhou, X. Yang, L. He, Z. M. Hao, W. Luo, B. Xiong, X Xu, C. J. Niu, M. Y. Yan and L. Q. Mai, *Appl. Phys. Lett.*, 2015, 106, 111908.

33 Z. L. An, L. He, M. Toda, G. Yamamoto, T. Hashida and T. Ono, *Microsyst. Technol.*, 2014, 20: 201-208.

34 L. He, M. Toda, Y. Kawai, H. Miyashita, M. Omori, T. Hashida, R. Berger, T. Ono, *Nanotech.*, 2015, 26: 195601.